



UNIVERSITÀ POLITECNICA DELLE MARCHE  
Repository ISTITUZIONALE

On the dynamics in the southeastern Ligurian Sea in summer 2010

This is a pre print version of the following article:

*Original*

On the dynamics in the southeastern Ligurian Sea in summer 2010 / Poulain, P. -M.; Mauri, E.; Gerin, R.; Chiggiato, J.; Schroeder, K.; Griffa, A.; Borghini, M.; Zambianchi, E.; Falco, P.; Testor, P.; Mortier, L.. - In: CONTINENTAL SHELF RESEARCH. - ISSN 0278-4343. - ELETTRONICO. - 196:(2020).  
[10.1016/j.csr.2020.104083]

*Availability:*

This version is available at: 11566/290375 since: 2024-04-10T15:35:43Z

*Publisher:*

*Published*

DOI:10.1016/j.csr.2020.104083

*Terms of use:*

The terms and conditions for the reuse of this version of the manuscript are specified in the publishing policy. The use of copyrighted works requires the consent of the rights' holder (author or publisher). Works made available under a Creative Commons license or a Publisher's custom-made license can be used according to the terms and conditions contained therein. See editor's website for further information and terms and conditions.

This item was downloaded from IRIS Università Politecnica delle Marche (<https://iris.univpm.it>). When citing, please refer to the published version.

(Article begins on next page)

# Continental Shelf Research

## On the dynamics in the southeastern Ligurian Sea in summer 2010

--Manuscript Draft--

<b>Manuscript Number:</b>	
<b>Article Type:</b>	Research paper
<b>Section/Category:</b>	Physical Oceanography (estuarine, coastal and shelf sea - modelling and process studies)
<b>Keywords:</b>	Drifter, glider, Ligurian Sea, Corsica Channel, offshore-flowing filaments, wind-driven circulation
<b>Corresponding Author:</b>	Pierre-Marie Poulain OGS Sgonico, Trieste Italy
<b>First Author:</b>	Pierre-Marie Poulain
<b>Order of Authors:</b>	Pierre-Marie Poulain Elena Mauri Riccardo Gerin Jacopo Chiggiato Katrin Schroeder Annalisa Griffa Mireno Borghini Enrico Zambianchi Pier Paolo Falco Pierre Testor Laurent Mortier
<b>Abstract:</b>	<p>Drifters and a glider were operated in the southeastern Ligurian Sea to study the near-surface currents and water mass properties in summer 2010. Additional data were collected by a moored current meter in the Corsica Channel (CC). These in situ data were complemented by surface wind products, satellite images of chlorophyll concentration and a Regional Ocean Modeling System (ROMS) numerical model that was implemented to simulate the local coastal dynamics. Southward currents were prevailing along the continental Italian coast, advecting filaments with a high optical signal coming from the Arno River. North of Elba Island, currents turned westward and northward in the vicinity of the CC. Further to the north they veered eastward, forming an anticyclonic circulation feature centered around Capraia Island. This general circulation picture was disrupted and reversed during events of sustained southerly winds occurring with a period of about a week. The near-surface currents in the CC and the anticyclonic circulation around Capraia Island showed the same weekly variations related to the local wind forcing. The ROMS model simulations agreed satisfactorily with the observations, in particular the strength of the Capraia anticyclonic circulation (quantified with the Capraia index) was confirmed to be strongly wind-dependent.</p>
<b>Suggested Reviewers:</b>	Hezi Gildor hezi.gildor@mail.huji.ac.il Dan Hayes hayesdan@cyprus-subsea.com Nadia Pinardi nadia.pinardi@unibo.it Carlo Brandini brandini@lamma.rete.toscana.it



Sgonico, 13 September 2019

Dear Sir/Madam:

Please find attached a manuscript entitled "On the dynamics in the southeastern Ligurian Sea in summer 2010" that we would like to be considered for publication in the Continental Shelf Research.

Sincerely yours.

Dr. Pierre-Marie Poulain

Head, Mobile Autonomous Oceanographic Systems (MAOS)  
Oceanography Section, OGS  
Senior Scientist  
Environmental Knowledge and Operational Effectiveness (EKOE), CMRE

1  
2  
3  
4  
5  
6  
7  
8  
9  
10  
11  
12  
13  
14  
15  
16  
17  
18  
19  
20  
21  
22  
23  
24  
25  
26  
27  
28

## On the dynamics in the southeastern Ligurian Sea in summer 2010

<sup>1,2</sup>Poulain P.-M., <sup>1</sup>Mauri E., <sup>1</sup>Gerin R., <sup>3</sup>Chiggiato J., <sup>3</sup>Schroeder K., <sup>4</sup>Griffa A., <sup>4</sup>Borghini M.,  
<sup>5,6</sup>Zambianchi E., <sup>5</sup>Falco P., <sup>7</sup>Testor P., <sup>7</sup>Mortier L.

<sup>1</sup>Istituto Nazionale di Oceanografia e di Geofisica Sperimentale (OGS), Trieste, Italy

<sup>2</sup>Center for Maritime Research and Experimentation (CMRE), La Spezia, Italy

<sup>3</sup>Istituto di Scienze Marine (ISMAR), CNR, Venezia, Italy

<sup>4</sup>Istituto di Scienze Marine (ISMAR), CNR, La Spezia, Italy

<sup>5</sup>Università Parthenope, Naples, Italy

<sup>6</sup>Istituto di Scienze Marine (ISMAR), CNR, Rome, Italy

<sup>7</sup>Laboratoire d'Océanographie et du Climat (LOCEAN), Paris, France

Corresponding author:

P.-M. Poulain,  
OGS, Borgo Grotta Gigante, 40/c,  
Sgonico (TS), Italy  
(ppoulain@inogs.it)

Continental Shelf Research

September 2019

**Keywords:** Drifter, glider, Ligurian Sea, Corsica Channel, offshore-flowing filaments,  
wind-driven circulation

## Highlights

29

30

31

- The surface circulation in the southeastern Ligurian Sea is strongly wind-dependent.

32

33

- Anticyclonic circulation around Capraia Island is predominant.

34

- Currents transport offshore filaments of low-salinity and nutrient-rich waters of riverine origin.

35

36

## **Abstract**

37

38

Drifters and a glider were operated in the southeastern Ligurian Sea to study the near-surface currents and water mass properties in summer 2010. Additional data were collected by a moored current meter in the Corsica Channel (CC). These in situ data were complemented by surface wind products, satellite images of chlorophyll concentration and a Regional Ocean Modeling System (ROMS) numerical model that was implemented to simulate the local coastal dynamics. Southward currents were prevailing along the continental Italian coast, advecting filaments with a high optical signal coming from the Arno River. North of Elba Island, currents turned westward and northward in the vicinity of the CC. Further to the north they veered eastward, forming an anticyclonic circulation feature centered around Capraia Island. This general circulation picture was disrupted and reversed during events of sustained southerly winds occurring with a period of about a week. The near-surface currents in the CC and the anticyclonic circulation around Capraia Island showed the same weekly variations related to the local wind forcing. The ROMS model simulations agreed satisfactorily with the observations, in particular the strength of the Capraia anticyclonic circulation (quantified with the Capraia index) was confirmed to be strongly wind-dependent.

53

54 **1. Introduction**

55 Currents and transports of water mass properties in sea areas including islands and channels  
56 and in the coastal zone are crucial at the local scale for the dispersion and mixing of pollutants  
57 and at the large scale for the interaction between different basins, which in turn can control  
58 the whole functioning of entire seas or oceans. Besides, if important river mouths co-exist in  
59 the vicinity of islands and channels, the distribution of the water masses and the local  
60 ecosystem dynamics can even be more complex and challenging to monitor and study.

61

62 The Mediterranean area in the southeastern Ligurian Sea and northern Tyrrhenian Sea (Fig.  
63 1), connected by the Corsica Channel (CC), is such an area, with complex topography and  
64 coast morphology, the existence of several islands (Elba, Monte Cristo, Giglio, etc) and also  
65 the mouth of an important Italian river (the Arno River). Fluxes across the CC have been  
66 measured almost continuously between 1982 and 1998 with moored currentmeters (Manzella,  
67 1984; Astraldi et al., 1990; Astraldi and Gasparini, 1992). The northward flowing current in  
68 the CC, also referred to as the Tyrrhenian (Astraldi and Gasparini, 1992) or Eastern Corsica  
69 Current (ECC, Pinardi et al. 2006), is maximum in winter and is mainly driven by the steric  
70 sea level difference between the Tyrrhenian to the south and the Ligurian Sea to the north.  
71 This difference is larger in winter due to the larger heat loss and the local effect of the wind  
72 stress curl in the Liguro-Provençal basin (Pinardi and Masetti, 2000). The heat flux  
73 associated with the ECC varies seasonally and plays a crucial role for deep water formation  
74 processes in the NW Mediterranean (Astraldi and Gasparini, 1992). The ECC is characterized  
75 by velocity fluctuations with periods between 2 and 15 days with the occurrence of  
76 intermittent reversals (Astraldi et al., 1990).

77

78 This ECC seasonal (and also inter-annual) variability was confirmed by satellite altimetry  
79 data along selected satellite sub-tracks criss-crossing in the CC vicinity (Vignudelli et al.,

80 1999, 2000, 2005; Bouffard et al., 2008). Vignudelli et al. (1999) have shown that the  
81 interannual variations of water transport through the CC, as measured by satellite altimeters,  
82 can be related to the North Atlantic Oscillation. More recently, Bouffard et al. (2008) have  
83 demonstrated that multi-mission altimetric data agree well with in-situ measurements and  
84 therefore represent an accurate long-term mean to monitor the exchange between the  
85 Tyrrhenian and Ligurian seas.

86

87 Conductivity-temperature-depth (CTD) measurements and numerical simulations (Onken et  
88 al., 2005) as well as surface drifters (Poulain et al., 2012) have shown that the ECC can veer  
89 in the clockwise sense around Capraia Island and form an anticyclonic eddy centered around  
90 the island. We will refer to this circulation feature as the Capraia anticyclone, although it has  
91 recently been also named “Ligurian Anticyclone” by Ciuffardi et al. (2016). It appears to be  
92 dominant in summer when the ECC is weak. In particular, one drifter in summer 2007  
93 completed 5 full loops around the island with a periodicity of about 3 days (Poulain et al.,  
94 2012).

95

96 In this paper, simultaneous observations of currents and water mass properties obtained by a  
97 glider, surface drifters and moored instruments, along with ancillary satellite data and wind  
98 products and numerical model simulations, are used to explore and study the dynamics of the  
99 southeastern Ligurian and CC in summer 2010. Most data were collected as part of the  
100 LIDEX10 campaign, whose general objective was to improve the understanding of turbulent  
101 transport and dispersion in the ocean, more specifically to study the dispersion in a coastal  
102 frontal zone due to mixing by meso- and submesoscale structures (Schroeder et al., 2012).  
103 The main focus of this paper is on mesoscale (~10 km) and submesoscale (< 10 km)  
104 structures, some of them transporting offshore and mixing the fresh and nutrient-rich waters  
105 of river origin. The Capraia anticyclone, which has a subbasin scale (40-50 km), is described

106 quantitatively using the drifter data. Some aspects of the near-surface circulation and ECC  
107 transport are also investigated, relating them to the local wind forcing.

108

109 Details about the instruments used and the collected data are provided in section 2. The  
110 surface circulation as measured by the drifters is described in section 3.1, including a  
111 qualitative description of their motions and a quantitative study of the Capraia anticyclone.  
112 The effect of the local wind forcing is explored in section 3.2, using both observations and  
113 numerical simulations obtained with the Regional Ocean Modelling System (ROMS). The  
114 surface circulation derived from ocean color satellite images superimposed with drifter tracks  
115 is discussed in section 3.3. Section 3.4 includes the results on the 3D spatial structure and  
116 temporal evolution of the water mass properties (temperature and salinity) provided by the  
117 glider and also detected in ocean color satellite images. Discussion of the most salient results  
118 and conclusions are found in section 4.

119

## 120 **2. Data and methods**

121 The LIDEX10 experiment took place on-board the R/V Maria Grazia of the Italian National  
122 Research Council (CNR) on 3 July 2010 in the southeastern Ligurian Sea off the Tuscany  
123 coast (Italy). First, a conductivity-temperature-depth (CTD) survey was carried on, along a  
124 zonal transect at latitude  $43^{\circ} 35.34'$  N and between longitudes  $9^{\circ} 56.7'$  E and  $10^{\circ} 5.94'$  E,  
125 including 12 casts down to 50 m depth and separated by 1-4 km. The CTD data revealed a  
126 near-surface vertical front in the top 7-8 m below the surface, separating lower salinity and  
127 higher chlorophyll fluorescence water inshore from saltier and poorer water offshore  
128 (Schroeder et al., 2012). The CTD data are not discussed any further in this paper since the  
129 glider repeated the same transect shortly after.

130

131        *2.1 In-situ observations*

132        2.1.1 Drifters

133

134        Two groups of 9 drifters were deployed after the CTD transect on 3 July 2010, on each side of  
135        the front, approximately 5 km apart. For each group, the drifters were released in three tight  
136        triplets separated by 300-500 m, and with 50-100 m distance between the drifters within each  
137        triplet (see Fig. 2 of Schroeder et al., 2012). An additional drifter was deployed between the 2  
138        groups on the front. In brief, the 19 drifters were deployed with relative distances ranging  
139        from 50 m to 6 km. The deployments were conducted in less than 4 h (from 11:34 to 15:26  
140        GMT). All drifters were CODE designs (Poulain, 1999; Poulain and Gerin, 2019), fitted with  
141        GPS receivers and manufactured by Technocean (Cape Coral, Florida). They measure the  
142        currents in the top first meter below the surface with an accuracy of 1-2 cm/s. The principal  
143        error is a wind-induced slip of about 0.1% of the wind speed (Poulain and Gerin, 2019). Most  
144        of the drifters (17 units) transmitted their data to the Argos system on-board polar-orbiting  
145        satellites, whereas 2 drifters used the Iridium telemetry system. GPS positions and ancillary  
146        data (e.g., sea surface temperature, battery voltage) were transmitted every hour.

147

148        The drifter GPS data were quality controlled and interpolated at 0.5 h intervals using a kriging  
149        technique (see Menna et al., 2017 and references therein). Velocities were calculated by finite  
150        differencing the interpolated positions (central difference scheme with hourly interval). For  
151        some applications (see section 3.2) the drifter velocity timeseries were low-pass filtered with a  
152        Hamming filter (36 h) to remove high frequency motions.

153

154        The mean half-life of the 19 drifters deployed on 3 July 2010 is about 2 weeks (many drifters  
155        stopped on 19-21 July after 16-18 days). Unfortunately, the single drifter deployed between  
156        the two clusters was rather short lived and stopped functioning on 7 July.

157

### 158 2.1.2 Glider

159 A shallow water Slocum glider manufactured by Teledyne Webb Research, Falmouth,  
160 Massachusetts was deployed at location  $43^{\circ} 35.78' N$ ,  $10^{\circ} 06.20' E$  on 3 July 2010, shortly  
161 after the drifter deployments (i.e., at 16:29 GMT). The glider was equipped with an un-  
162 pumped Sea-Bird Scientific SBE 41 CT to measure conductivity (0.0003 S/m), temperature  
163 ( $0.002^{\circ} C$ ) and pressure (0.5 psi), along with sensors to measure dissolved oxygen, particle  
164 backscattering and coloured dissolved organic matter fluorescence. It was programmed to  
165 measure vertical properties of the water column as deep as 200 m. All sensors were set to  
166 record every 8 seconds. The typical horizontal resolution of the glider data along its route was  
167 about 0.5 km. In this paper only temperature, salinity and density observations are considered  
168 to describe the local dynamics, with a main focus on the top 40 m of water.

169

170 The glider was initially piloted to sample the transect surveyed by the research vessel. Given  
171 the southward motion of the drifters, and in order to have the glider and drifters in the same  
172 area at about the same time, the glider was subsequently programmed to survey the  
173 southeastern Ligurian Sea in a southward zig-zag pattern until it approached the northern  
174 coast of Elba Island (Fig. 1). At this point it was piloted to move westward and to sample the  
175 CC, until it was recovered on 20 July 2010 (at about 10:00 GMT) at  $43^{\circ} 00.90' N$ ,  $09^{\circ} 35.82'$   
176 E, between the northern tip of Corsica and Capraia Island.

177

### 178 2.1.3 Mooring

179 A mooring with current meters is maintained by CNR ISMAR in the CC (between the  
180 northern tip of Corsica and Capraia Island) since 1985. Its location is  $43^{\circ} 1.5' N$ ,  $9^{\circ} 41.0' E$ .  
181 Current profiles are measured with an upward 75 KHz RDI Acoustic Doppler Current Profiler  
182 (ADCP), with a bin size of 16 m, between 32 and 384 m at 2 h intervals. The meridional and

183 zonal velocities were extracted from the dataset for the period July-August 2010. Only the  
184 meridional (along-channel) component is considered here, since it is more significant for our  
185 scopes than the zonal (across-channel) component (the meridional speed is on average 3 times  
186 stronger than the zonal one), and gives indication on the water exchange between the  
187 Tyrrhenian and the Ligurian Sea. For comparison with the surface drifter data, the mooring  
188 data near 32 m depth was considered. In order to remove high frequency fluctuations, a  
189 Hamming filter with cut off period of 36 h was applied to the velocity time series.

190

### 191 *2.2 Remotely sensed data*

192 Moderate Resolution Imaging Spectroradiometer (MODIS) satellite images of chlorophyll  
193 concentration of the study area were used to describe the spatial structure and temporal  
194 evolution of the surface circulation assuming that chlorophyll is a passive tracer advected by  
195 the surface horizontal currents. Images of chlorophyll concentration were preferred on sea  
196 surface temperature images as they delineate better the circulation features at meso- and  
197 submesoscales (better contrast). Being in a coastal area where a river outflows nutrient-rich  
198 water, there is a sharp contrast between coastal and offshore waters, the former being richer  
199 (higher chlorophyll) and slightly colder (by about 1 °C, in our case). The daily images have a  
200 horizontal resolution of 1 km.

201

### 202 *2.3 Wind products*

203 Consortium for Small-scale Modeling (COSMO, <http://www.cosmo-model.org>) wind  
204 products run by the Italian Air Force National Meteorological Center were obtained for the  
205 study area in July and August 2010. In particular, the COSMO-ME gridded 10-m vector  
206 winds with 7 km grid spacing were used to force the ROMS model and to relate the wind  
207 forcing to the currents measured by the drifters and at the CC mooring. For some applications  
208 (see section 3.2) the COSMO-ME wind velocity timeseries were also low-pass filtered with a

209 Hamming filter (36 h) to remove high frequency fluctuations. Wind data at 10-m were also  
210 obtained from the ODAS buoy (also called W1-M3A) located in the central Ligurian Sea (43°  
211 48' N, 9° 9.6' E).

212

## 213 *2.4 Numerical simulations*

214 The ocean model employed in this application is the ROMS (Haidvogel et al., 2008;  
215 Shchepetkin and McWilliams, 2005). As part of LIDEX10, the model was set up in  
216 operational forecast mode on a domain covering the entire Ligurian Sea. The horizontal  
217 resolution is 2 km, with 32 vertical sigma-levels non-linearly stretched to resolve the surface  
218 boundary layer. The ocean model was forced by the COSMO-ME 10-m winds. Open  
219 boundary conditions were applied to tracers and baroclinic velocity with radiation and  
220 nudging (Marchesiello et al. 2001) from daily averages of the large-scale Mediterranean  
221 Forecasting System (MFS) forecasts (Oddo et al., 2009). Three major rivers were included:  
222 the Arno (daily discharges), Serchio and Magra (monthly climatologies). The operational  
223 ROMS-based system was initialized on 1 May 2010 using an analysis field from the  
224 Mediterranean Forecasting System (MFS) model. Since then, ROMS was run in forecast  
225 mode once a day (00:00 UTC) with output data every 3 h and forecast range of 72 h. Data  
226 assimilative analysis fields from the forecast system are available in Mourre and Chiggiato  
227 (2014), but just for a short period. Thus, for this work only the free run (i.e., without data  
228 assimilation) is considered. Additional details on the physics and numerical details  
229 implemented in this application and performance can be found in Alvarez et al. (2012),  
230 Schroeder et al. (2012), Mourre et al. (2011) and Mourre and Chiggiato (2014).

231

## 232 **3. Results**

### 233 *3.1 Surface circulation*

234

235 After deployment, all drifters moved southward, with the coastal group (red tracks in Fig. 2)  
236 going faster and reaching 43°N latitude after 4 days, on 7 July. The other group (blue tracks in  
237 Fig. 2) followed with about 1-day delay. Between 7 and 10 July the coastal group proceeded  
238 westward towards the CC, and veered southward upon approaching Corsica. In contrast, the  
239 other drifters slowed down and stagnated just north of Elba Island for about 2 days (11-12  
240 July). Most of these drifters then moved northward (in the ECC and also near the Italian  
241 continental coast) on 13-14 July, before turning back and moving south and west starting on  
242 15 July. On 15-19 July, the drifters in the southern part of the CC showed slow and rather  
243 chaotic currents, except for 2 drifters which moved swiftly northward between the northern tip  
244 of Corsica and Capraia Island on 14 and 19 July. Four drifters (blue tracks) moved to the  
245 southwest rapidly on 19 July and joined the area of the CC.

246

247 After the recovery of the glider on 20 July, some drifters continued to provide data on the  
248 surface circulation in the study area for about another month (not shown). The most striking  
249 characteristics of the currents during that period are: 1) on 22 July, fast northward currents in  
250 the CC; 2) on 23-25 July, reversal of this current with drifter moving south in the CC; and 3) a  
251 prevailing anticyclonic circulation around Capraia Island mostly during the period 20 July -  
252 17 August. No drifter moved north of 43° 30' N and only 3 drifters moved eventually to the  
253 Tyrrhenian Sea south of 42° 30' N after some time. The composite plot of all the drifter  
254 trajectories between 3 July and 27 August 2010 is shown in Fig. 3, with speed color-coded  
255 along the trajectories. Fastest unfiltered currents reaching 90 cm/s occur north of the CC in  
256 the ECC (near 43° 15' N). Southward currents sampled during the first few days after  
257 deployment range in 30-40 cm/s. Currents in the anticyclonic circulation around Capraia  
258 Island are mostly in the 30-60 cm/s range. In the “stagnant” areas north of Elba Island and in  
259 the CC, the speed is bounded by 20 cm/s. Note that high frequency motions, shown as loops  
260 in the tracks, are ubiquitous in most of the drifter data. These motions have speeds of 10-20

261 cm/s. Spectral analysis revealed that they correspond to near-inertial oscillations, tidal  
262 motions and currents driven by sea breeze. These high frequency motions are not considered  
263 in the rest of the paper since the main focus is on dynamics at meso- and submesoscales.

264

265 Pseudo-Eulerian statistics were calculated from the drifter data for the period 3 July to 27  
266 August 2010 using bins of  $0.05^\circ$  latitude  $\times$   $0.05^\circ$  longitude. The number of hourly drifter  
267 observations in the bins is maximum (in excess of 500) north of Elba Island and in the  
268 southern part of the CC (not shown). Mean currents are shown in Fig. 4. for bins with more  
269 than 5 hourly observations. The strong anticyclonic circulation around Capraia Island is  
270 striking with mean speeds reaching 30 cm/s. This feature is about 60-70 km in diameter and is  
271 bounded by  $9^\circ 30'$  E and  $10^\circ 20'$  E in longitude and  $42^\circ 50'$  N and  $43^\circ 30'$  N in latitude. Its  
272 center is just to the northeast of Capraia Island. The period of rotation is 5-10 days. In total,  
273 eight drifters executed 13 loops in this structure between 19 July and 19 August (one month).  
274 Two drifters executed 4 loops each.

275

276 Fig. 5 shows the geographical distribution of the variability of the surface currents with  
277 respect to the mean pattern shown in Fig. 4. The eddy kinetic energy (see definition in  
278 Poulain, 2001) is low in the eastern part of the study area and in the southern CC. It increases  
279 near the northern tip of Corsica and the northern extension of the CC (in the ECC) and the  
280 northern limb of the anticyclonic circulation around Capraia Island.

281

### 282 *3.2 Wind forcing, near-surface currents and numerical simulations*

283 The COSMO-ME wind products at the grid point nearest the CNR mooring in the CC ( $43^\circ$   
284  $7.5'$  N,  $9^\circ 37.5'$  E, see Fig. 1) were considered to study the variability of the near-surface  
285 currents related to the wind forcing. As shown in Fig. 6, in addition to daily variations  
286 corresponding to sea breeze (see thin curve in middle panel), the wind is alternating between

287 northerly and southerly regimes with a periodicity of about a week. More specifically, major  
288 northerly wind events occurred on 19, 24 and 30 July and on 6 and 21 August. On 14, 22 and  
289 29 July and 15-16 and 27 August, winds were primarily southerly. Fig. 6 shows that the low-  
290 pass filtered currents at 32 m depth measured by the mooring in the CC respond to the local  
291 wind forcing, i.e., major events of southerly (northerly) winds correspond to increased  
292 northward (southward) velocity. The correlation with zero-time lag between the meridional  
293 winds and currents is about 0.69, but it increases to 0.71 for a lag of 5 h. This means that the  
294 currents are barely delayed with respect to the wind.

295

296 If we plot the low-pass filtered drifter meridional velocities versus time along with the low-  
297 pass filtered near-surface meridional flow in the Corsica Channel (Fig. 6, bottom panel), it is  
298 striking that most drifter speeds co-vary with the mooring data. In particular, during the  
299 events of strong northward flow (and southerly winds) of 13-14, 22-23 and 28-29 July, most  
300 drifters are moving northward with speeds up to about 50 cm/s (after low-pass filtering). On  
301 18-19, 23-24 and 29-30 July under northerly wind forcing the majority of drifters are moving  
302 southward and the upper current in the CC is reversed (southward). Note that the variance of  
303 the drifter meridional velocity is much higher than the mooring data mostly due to the spatial  
304 variability sampled by the drifters.

305

306 Fig.7 shows the average surface circulation in the Ligurian Sea in July - August 2010  
307 produced by ROMS. The two-month average clearly suppresses all short-term variability and  
308 the emerging picture is controlled by the permanent features in the area. The overall  
309 circulation of the western Ligurian Sea is cyclonic. Surface Atlantic Water (AW) enters the  
310 Ligurian Sea from the south, mostly from the Algerian basin through the Western Corsica  
311 Current (WCC). As expected in summer, the ECC in the CC is weak, in good agreement with  
312 the drifter data (Fig. 4). The resulting current proceeds northward as a geostrophic frontal

313 system becoming the so-called Northern Current (NC) in the northern Ligurian Sea. In the  
314 eastern Ligurian Sea, the Capraia anticyclone, identifiable in Fig. 7 by the relative maximum  
315 in sea surface elevation, was a robust permanent feature of summer 2010.

316

317 In order to test the relationship with wind impulses, a Capraia Index was defined as the  
318 difference in sea surface elevation between points A and B (see location in Fig. 7, top panel);  
319 thus, a value close to zero corresponds to a wide shelf current whereas a large positive value is  
320 suggestive of a strong anticyclone. The choice of an index that included point C (see Fig. 7)  
321 was discarded, as the difference in sea surface elevation with respect to A may be due to a  
322 structured boundary current (i.e., the WCC) disregarding the existence of the anticyclone.  
323 From the time-series of the Capraia index (Fig. 7, middle panel) it can be seen that (a) the  
324 anticyclone grows in intensity from early July to the end of August and (b) significant wind  
325 events have the ability to partially or totally suppress the feature, with the noticeable example  
326 of the (southwesterly) storm on 14-15 August (see wind speed in Fig. 7 bottom panel). As the  
327 wind impulse weakens however, the index is suggestive of a re-emergence of the feature. The  
328 southerly wind event around 13-14 July is in good agreement with the reversal of the coastal  
329 current revealed by the drifters (Fig. 2).

330

### 331 *3.3 Surface circulation and satellite images*

332

333 During the period of glider operation (3-20 July) only 8 MODIS images were partially cloud  
334 free and provided a useful description of chlorophyll concentration and the associated near-  
335 surface circulation. On the day of the drifter and glider deployments (3 July), there was a  
336 rather well-developed area of water with high chlorophyll concentration off the continental  
337 Italian coast from the Arno River mouth to about 43°N 15' (Fig. 8a). This increased optical  
338 signal is related to the higher nutrients discharged by the river. The significant Arno plume

339 was probably the result of an event on high discharge rate (reaching nearly 200 m<sup>3</sup>/s) around  
340 21 June 2010 (data courtesy of Regione Toscana). The image confirms that the two groups of  
341 9 drifters were deployed in and outside the coastal layer. The next two days (4 and 5 July, Fig.  
342 8b,c), while all drifters were moving southward, the coastal layer developed two instabilities  
343 forming offshore-flowing (and also southward flowing) filaments near 43° 25' N and 43° 10'  
344 N. On 8 July (Fig. 8d), these instabilities were well separated in latitude and showed cyclonic  
345 veering, that is offshore and southward circulation. The rich water of the southern instability  
346 was advected towards Elba Island and then westward towards Corsica. There is a particularly  
347 good agreement between the chlorophyll structures and the drifter tracks.

348

349 The offshore-flowing instabilities rooted on the Italian continental coast were still present  
350 between 10 and 19 July (Fig. 9) with various shapes and offshore extensions. The northern  
351 one extended as far as the Gorgona Island. Others developed near and south of Elba Island,  
352 but were away from the areas sampled by the drifters and glider. To the west, off Corsica, an  
353 instability plume was evident on 12, 17 and 19 July (Fig. 9b,c,d). On 12 July (Fig. 9b) drifters  
354 were even trapped in it as it developed more offshore (as far as east as 9° 45' E).

355

356 During its entire mission, the glider protruded in and out of the chlorophyll-rich waters. For  
357 instance, on 8 July (Fig. 8d) it encountered richer waters near the surface at both extremities  
358 of this southwestward transect.

359

### 360 *3.4 Water mass properties and geostrophic currents in the water column*

361

362 The distribution of temperature, salinity and density along the glider track is discussed here  
363 below, with main focus on the top 40 m of water where most of the variability occurs.  
364 Selected transect (1, 8 and 15, see location in Fig. 1) are considered for the sake of brevity.

365

366 During its entire operation, the glider revealed a near-surface mixed layer extending down to  
367 5-10 m (Figs. 10-12) on top of a thermocline spreading between approximately 10 and 40 m.  
368 Along the northernmost transect 1 (Fig. 10) the isotherms and isopycnals are inclined  
369 (deepening going offshore to the W) and the corresponding geostrophic currents are directed  
370 southward. Further to the south, along transect 8 (Fig. 11), the above-mentioned iso-curves  
371 are characterized by a concave upward structure. Qualitatively, the geostrophic currents are to  
372 the SW in the eastern portion, where the drifters also move to the S and SW (see Fig. 8d).  
373 More offshore (to the W) the currents are reversed, thus representing a mesoscale anticyclonic  
374 circulation feature. In the southern part of the CC, along the zonal transect 15 (Fig. 12), the  
375 isotherms and isopycnals correspond to concave downward. Again this is compatible with the  
376 southward motion of the drifters near Corsica, and the usual northward direction of the ECC,  
377 which is rather weak in summer.

378

379 Low-salinity water of Arno River origin (as demonstrated before in satellite images) extends  
380 almost across the entire section but most importantly for distances larger than 2 km from the  
381 westernmost point (Fig. 10). Water with salinity less than 37.6 prevails in the top 5-m layer.  
382 Below it, the salinity is gradually increasing and reaching values in excess of 38.0 around 40  
383 m depth. This is a signature of the upper core of the Levantine Intermediate Water which can  
384 reach salinity of 38.6-38.7 at depths of 300-500 m in the Ligurian Sea (Bosse et al., 2015).  
385 Besides the above-described features, the high horizontal resolution of the glider allowed to  
386 sample a vein of relatively low salinity (~37.6) expanding offshore along transect 1 (Fig. 10)  
387 between 10 and 25 m depth. The inclination of the vein is compatible with the slope of the  
388 isopycnals and indicates the subduction of coastal water.

389

390 Along transect 8 the near surface salinity above 10 m has two minima (near 37.0) at the  
391 extremities, corresponding to the Arno River plume extending offshore (to the east), and  
392 presumably to the Atlantic Water coming from the CC (to the west). This low-salinity water  
393 is also seen in transect 15 across the CC, although a little bit deeper (5-10 m) and capped  
394 partially by saltier water.

395

396 In the CC (eastern part of transect 15), the glider data show consistent northward currents in  
397 the entire depth range (0-200 m) whereas the mooring currents (Fig. 13) show mostly  
398 northward currents above 80 m, with intensification on 13-14, 22 and 29 July and 14-15  
399 August. Below, there are 1-2 weeks long periods of flow reversal, the most prominent one  
400 lasting from 14 to 25 July and involving the water column up to 60 m depth. The surface  
401 northward velocities average was  $11.2 \pm 7.4$  cm/s, while the southward ones were much weaker  
402 ( $-2.8 \pm 2.6$  cm/s).

403

404

#### 405 **4. Discussion and conclusions**

406

407 During summer 2010, surface drifters and a glider were operated simultaneously to explore  
408 the dynamics of the southeastern Ligurian Sea where the wind forcing, the local  
409 geography/bathymetry and the outflow of the Arno River are supposed to affect significantly  
410 the circulation and the distribution of the water mass properties. The glider was piloted in  
411 order to obtain information in the water column in the area sampled by most of the drifters.  
412 Ancillary data were obtained from a permanent mooring in the CC and from satellites  
413 (MODIS images of chlorophyll concentration). In addition, a ROMS numerical model was  
414 used to simulate the local dynamics and to help with the interpretation of the collected data.

415

416 The drifters revealed a surface circulation strongly affected by the local winds. Southward  
417 currents dominated off the Italian continental coast. These currents reversed on 13-14 July due  
418 to a change in wind direction, changing to southerly. The fluctuation of surface currents  
419 between the southward and northward directions is seen in the drifter tracks over the entire  
420 study area (in particular in the vicinity of Capraia Island) and in the near-surface records of  
421 the mooring in the CC (see Fig. 6) during July and August 2010. The typical period of these  
422 oscillations is one week.

423

424 Some drifters eventually depicted a strong anticyclonic circulation pattern centered on  
425 Capraia Island (the Capraia anticyclone) starting on 20 July. The rotation period of these  
426 drifters is 5-10 days, that is, slightly longer than the value (3 days) reported by Poulain et al.  
427 (2012). Both drifters (Fig. 2) and the simulated sea surface height (Capraia index in Fig. 7)  
428 showed an enhancement of the Capraia anticyclone in late July and August, only interrupted  
429 by a storm on 14-15 August. This trend is related to the increase of negative vorticity of the  
430 winds from July to August (not shown). On 14-15 August, strong winds from the SW  
431 disrupted this trend and the anticyclone essentially vanished. In conclusion, ROMS numerical  
432 model successfully simulated the occurrence of the Capraia anticyclone as a semi-permanent  
433 and strengthening feature during July-August 2010, corroborating the hypothesis of the  
434 significant role played by wind-storms in perturbing this eddy as well as the surface  
435 circulation in the area.

436

437 The southward coastal currents advected the plume of the Arno River and associated  
438 filaments of nutrient-rich waters towards the south, forming a layer of high chlorophyll  
439 concentration along most of the Italian continental coast. This layer became unstable and  
440 offshore-flowing filaments were generated typically at two locations between the Arno mouth  
441 and Elba Island (see for instance Fig. 8d.). The northernmost filament reached almost the area

442 near Gorgona Island (Fig. 9d) and the southern one was advected near the northern coast of  
443 Elba Island, into the CC and around Capraia Island (Fig. 8c,d).

444

445 The temperature, salinity and density data provided by the glider between 3 and 20 July 2010  
446 show stratified conditions typical of summer with a surface mixed layer down to 10-20 m, a  
447 thermocline expanding down to a maximum depth of 40 m. In terms of salinity, horizontal  
448 variability (fronts) associated with the Arno plume and/or the AW occur along most transects.  
449 For the Arno plume and its extension into offshore-flowing filaments, there is a good  
450 agreement between the satellite chlorophyll images and the glider data. In the thermocline, an  
451 inclined intrusion of fresher water (probably of Argo River origin) observed in transect 1 (Fig.  
452 10) corresponds to subduction along isopycnals. Below 40 m, the increase of salinity with  
453 depth represents the upper part of the LIW.

454

455 Currents measured at the CNR mooring in the CC corroborated the fluctuations of the near-  
456 surface circulations with events of northward flow on 13-14, 22 and 29 July and 14-15 August  
457 also experienced by the drifters (Fig. 13). Deeper in the water column, southward reversing  
458 flow was observed for longer period (1-2 weeks) and rather independently from the surface  
459 variability. These flow reversal events have already been reported by Astraldi et al. (1990).  
460 They are not forced by the local winds but are probably related to the sea level difference  
461 between the Tyrrhenian and Ligurian Sea.

462

463 The combined use of data provided by mobile and fixed autonomous instruments (drifters,  
464 glider, mooring), by environmental satellites and numerical simulations in the southeastern  
465 Ligurian Sea exemplifies an efficient way of collecting oceanographic data in this complex  
466 sea area at relatively low costs. Obviously, a better sampling approach could have involved  
467 data collection with more than one glider, the deployment of fixed moorings at key locations,

468 and an extensive survey of the entire study area with a research vessel. The study of coastal  
469 dynamics as described in this paper, nevertheless, is a good example of multi-platform and  
470 multi-parameter approach, which is the future paradigm in observational oceanography.

471

## 472 **Acknowledgements**

473

474 The authors are grateful to all the people who helped with the drifter and glider  
475 deployment/recovery operations and with the data processing, and in particular to P. Zanasca,  
476 A. Bussani, M. Menna, I. Mancero-Mosquera and K. Mahiouz. The drifters used in LIDEX10  
477 were kindly provided by the NATO NURC Center (La Spezia, Italy), CNR, University  
478 Parthenope of Naples and OGS. The glider (TENUSE) was contributed by LOCEAN. The  
479 satellite data were downloaded from <https://modis.gsfc.nasa.gov/data/dataproduct/>. ODAS wind  
480 data were provided by the EU FP7 EuroSITES project. COSMO-ME data were kindly made  
481 available by CNMCA in Rome, Italy. Arno River data are courtesy of Servizio Idrologico –  
482 Regione Toscana. E. Z and P. F acknowledge support from the Parthenope University  
483 individual and group research funding.

484

485

486

487 **References**

488

489 Alvarez, A., Chiggiato, J., Mourre, B., 2012. Robotic characterization of access-restricted  
490 marine environments. *IEEE Rob. Autom. Mag.*, 20 (3), 42-49.

491

492 Astraldi, M., Gasparini, G.P., Manzella, G.M.R., Hopkins, T.S., 1990. Temporal variability of  
493 currents in the eastern Ligurian Sea, *J. Geophys. Res.*, 95(C2), 1515–1522.

494

495 Astraldi, M., Gasparini, G.P., 1992. The seasonal characteristics of the circulation in the  
496 North Mediterranean basin and their relationship with the atmospheric climatic conditions. *J.*  
497 *Geophys. Res.*, 97 (C6), 9531-9540.

498

499 Bosse, A., Testor, P., Mortier, L., Prieur, L., Taillandier, V., d’Ortenzio, F., Coppola, L.,  
500 2015. Spreading of Levantine Intermediate Waters by submesoscale coherent vortices in the  
501 northwestern Mediterranean Sea as observed with gliders, *J. Geophys. Res. Oceans*, 120,  
502 1599–1622, doi:10.1002/2014JC010263.

503

504 Bouffard, J., Vignudelli, S., Cipollini, P., Menard, Y., 2008. Exploiting the potential of an  
505 improved multimission altimetric data set over the coastal ocean, *Geophys. Res. Lett.*, 35,  
506 L10601, doi: 10.1029/2008GL033488.

507

508 Ciuffardi, T., Napolitano, E., Iacono, R., Reseghetti, F., Raiteri, G., Bordone, A., 2016.  
509 Analysis of surface circulation structures along a frequently repeated XBT transect crossing  
510 the Ligurian and Tyrrhenian Seas. *Ocean Dynam.*, 66(6–7), 767–83.

511

512 Haidvogel, D.B., Arango, H., Budgell, W.P., Cornuelle, B.D., Curchitser, E., Di Lorenzo, E.,  
513 Fennel, K., Geyer, W.R., Hermann, A.J., Lanerolle, L., Levin, J., McWilliams, J.C., Miller,  
514 A.J., Moore, A.M., Powell, T.M., Shchepetkin, A.F., Sherwood, C.R., Signell, R.P., Warner,  
515 J.C., Wilkin, J., 2008. Ocean forecasting in terrain-following coordinates: Formulation and  
516 skill assessment of the Regional Ocean Modeling System. *J. Comput. Phys.*, 227: 3595-3624.  
517

518 Manzella, G., 1985. Fluxes across the Corsica Channel and coastal circulation in the East  
519 Ligurina Sea. *Morth-Western Mediterranean*, *Ocean. Acta*, 8 (1), 29-35.  
520

521 Marchesiello, P., McWilliams, J. C., Shchepetkin, A. F., 2001. Open boundary conditions for  
522 long-term integration of regional oceanic models. *Ocean Modell.*, 3, 1–20.  
523

524 Menna, M., Gerin R., Bussani A., Poulain P.-M., 2017. The OGS Mediterranean Drifter  
525 Dataset: 1986-2016. *Rel. OGS 2017/92 Sez. OCE 28 MAOS*, OGS, Trieste, Italy.  
526

527 Moure, B., Chiggiato, J., 2014. A comparison of the performance of the 3-D super-ensemble  
528 and an ensemble Kalman filter for short-range regional ocean prediction. *Tellus A*, 66, 21640.  
529

530 Moure, B., Chiggiato, J., Lenartz, F., Rixen, M., 2012. Uncertainty forecast from 3-D super-  
531 ensemble multi-model combination: Validation and calibration. *Ocean Dynam.*, 62(2): 283-  
532 294.  
533

534 Oddo, P., Adani, M., Pinardi, N., Fratianni, C., Tonani, M., and Pettenuzzo, D., 2009. A  
535 nested Atlantic-Mediterranean Sea general circulation model for operational forecasting,  
536 *Ocean Sci.*, 5, 461-473, doi:10.5194/os-5-461-2009.  
537

538 Onken, R., Robinson, A.R., Kantha, L., Lozano, C.J., Haley, P.J., Carniel S. 2005. A rapid  
539 response nowcast/forecast system using multiply-nested Ocean models and distributed data  
540 systems, *J. Mar. Sys.*, 56, 45-66.  
541

542 Pinardi, N., Masetti, E. 2000. Variability of the large-scale general circulation of the  
543 Mediterranean Sea from observations and modelling: a review. *Palaeogeography,*  
544 *Palaeoclimatology, Palaeoecology*, 158, 153-173.  
545

546 Pinardi, N., Arneri E., Crise A., Ravaioli M., Zavatarelli M. 2006. The physical, sedimentary  
547 and ecological structure and variability of shelf areas in the Mediterranean Sea. In: A. R.  
548 Robinson and K. Brink (eds.), *The Sea*, Vol. 14 Harvard University Press, Cambridge, USA,  
549 1245-1330.  
550

551 Poulain, P.-M. 1999. Drifter observations of surface circulation in the Adriatic Sea between  
552 December 1994 and March 1996, *J. Mar. Syst.*, 20, 231-253.  
553

554 Poulain, P.-M. (2001), Adriatic Sea surface circulation as derived from drifter data between  
555 1990 and 1999, *J. Marine Sys.*, 29, 3-32.  
556

557 Poulain P.-M., Gerin R., Rixen M., Zanasca P., Teixeira J., Griffa A., Molcard A., De Marte,  
558 M., Pinardi N. 2012. Aspects of the surface circulation in the Liguro-Provençal basin and  
559 Gulf of Lion as observed by satellite-tracked drifters (2007-2009), *Boll. Geofis. Teor. Appli.*,  
560 53(2), 261-279.  
561

562 Poulain, P.-M. Gerin, R. 2019. Assessment of the water-following capabilities of CODE  
563 drifters based on direct relative flow measurements. *J. Atmos. Ocean Tech.*, 36(4), 621-633,  
564 doi: 10.1175/JTECH-D-18-0097.1

565

566 Vignudelli, S., Gasparini, G.P., Astraldi, M., Schiano, M.E. 1999. A possible influence of the  
567 North Atlantic Oscillation on the circulation of the Western Mediterranean Sea, *Geophys.*  
568 *Res. Lett.*, 26 (5), 623-626.

569

570 Vignudelli, S., Cipollini, P., Astraldi, M., Gasparini G.P., Manzella, G., 2000. Integrated use  
571 of altimeter and in situ data for understanding the water exchanges between the Tyrrhenian  
572 and Ligurian Seas. *J. Geophys. Res.*, 105 (C8), 19649-19663.

573

574 Shchepetkin, A.F., McWilliams, J.C., 2005. The regional ocean modelling system: a split-  
575 explicit, free-surface, topography-following-coordinates ocean model. *Ocean Modell.* 9, 347–  
576 404.

577

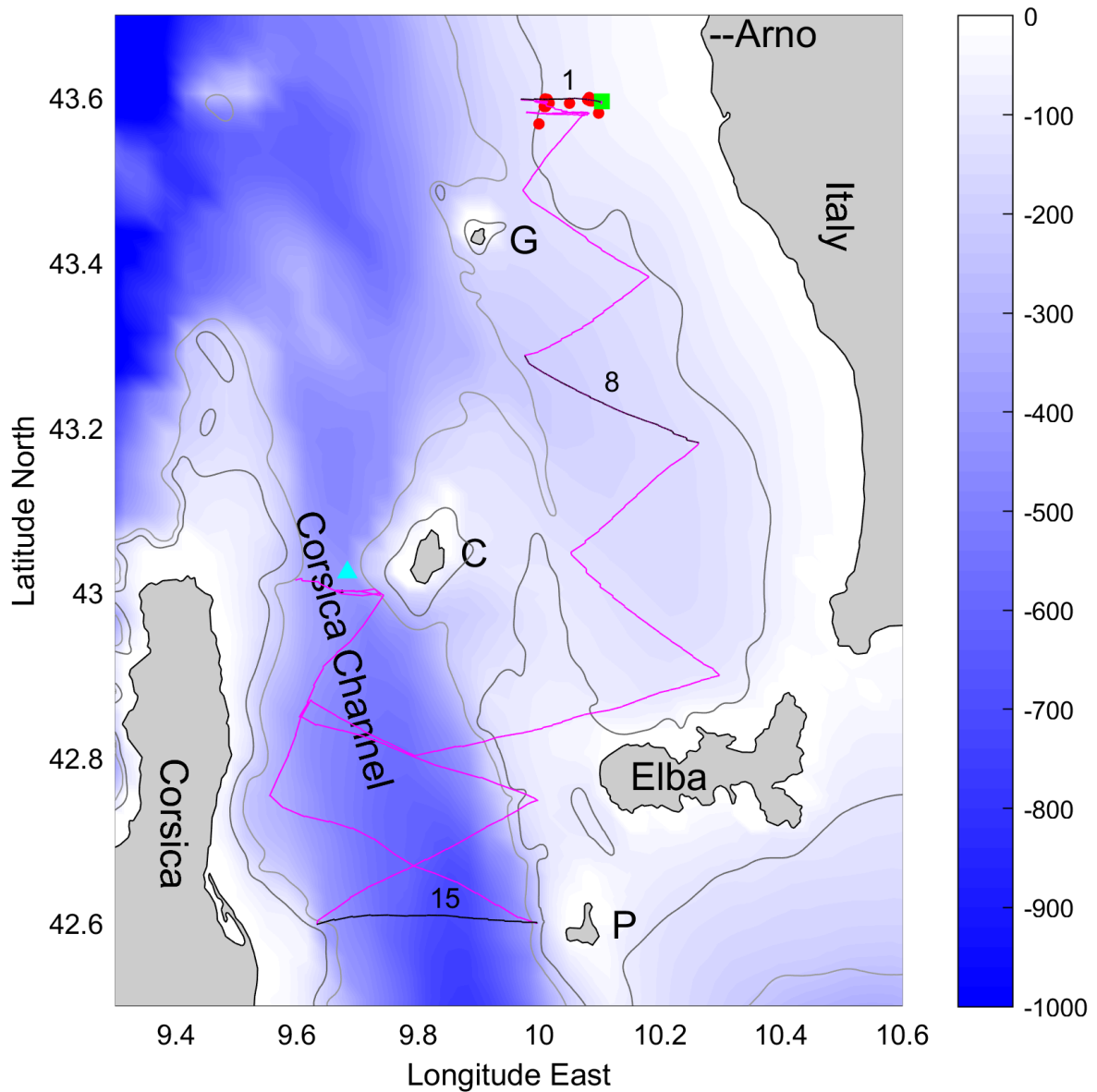
578 Vignudelli, S., Cipollini, P., Roblou, L., Lyard, F., Gasparini, G.P., Manzella G., Astraldi, M.  
579 2005. Improved satellite altimetry in coastal systems: Case study of the Corsica Channel  
580 (Mediterranean Sea), *Geophys. Res. Lett.*, 32, L07608, doi:10.1029/2005GL022602.

581

582 Schroeder, K., Chiggiato, J., Haza, A.C., Griffa, A., Özgökmen, T.M., Zanasca, P., Molcard,  
583 A., Borghini, M., Poulain, P.-M., Gerin, R., Zambianchi, E., Falco, P., Trees, C. 2012.

584 Targeted Lagrangian sampling of submesoscale dispersion at a coastal frontal zone. *Geophys.*

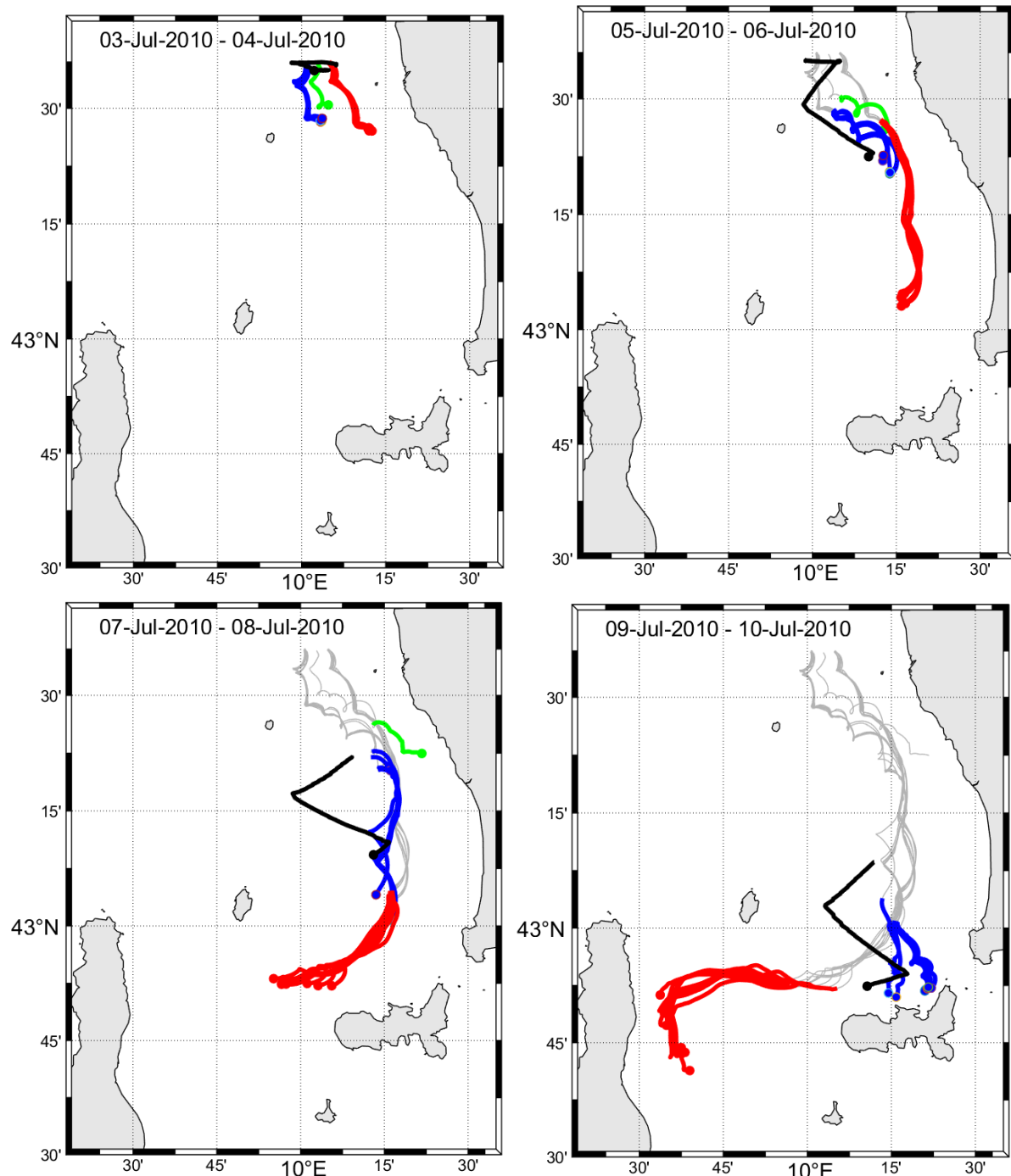
585 *Res. Lett.*, 39, L11608, doi:10.1029/2012GL051879.



586

587 Figure 1. Geography and bathymetry of the study area in the southeastern Ligurian and  
 588 Corsica Channel. The Gorgona (G), Capraia (C) and Pianosa (P) islands are shown in addition  
 589 to the Elba Island. The location of the CNR mooring is shown with a cyan triangle. The  
 590 deployment locations of the drifters (red dots) and glider (green square) are also indicated.  
 591 The glider track is shown in magenta, including the 3 transects (1, 8 and 15) described in the  
 592 paper. Bathymetry is contoured (100 and 200 m) and shown with blue shades (m).

593



594

595

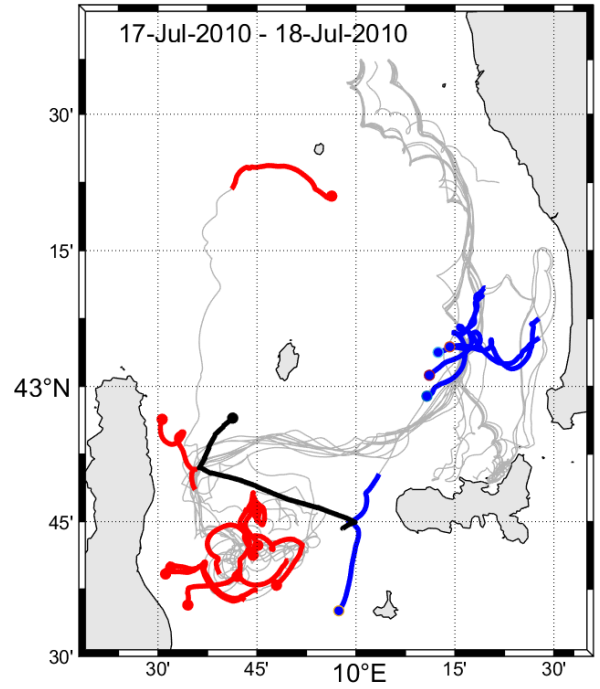
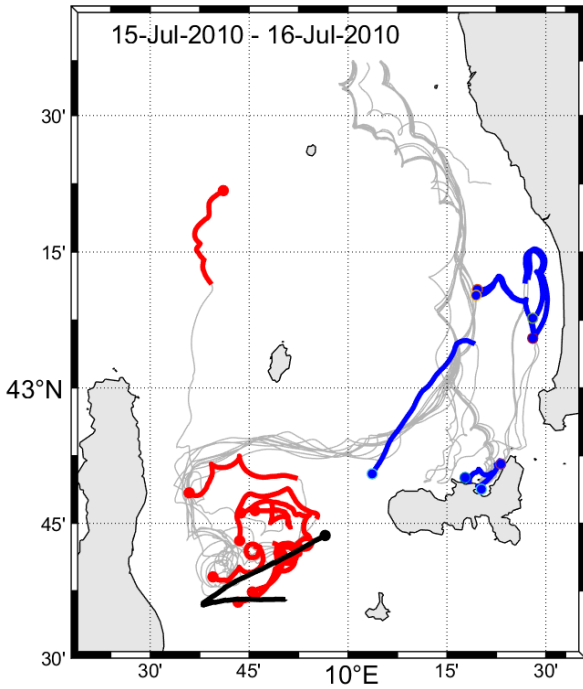
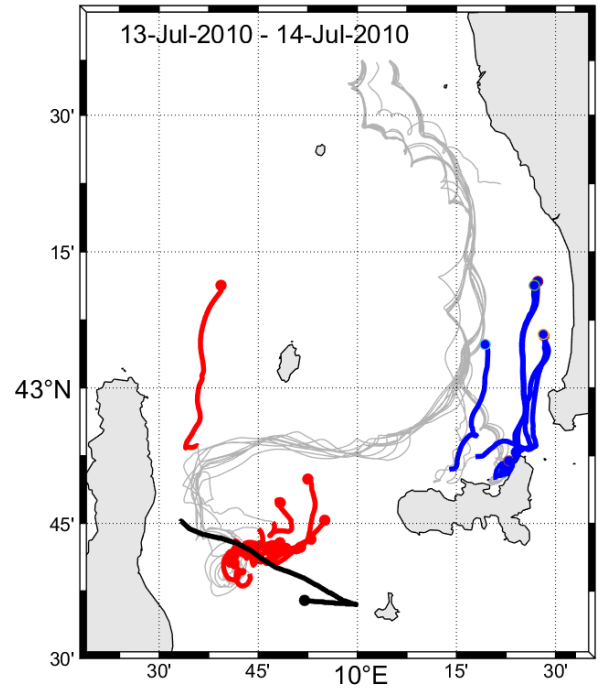
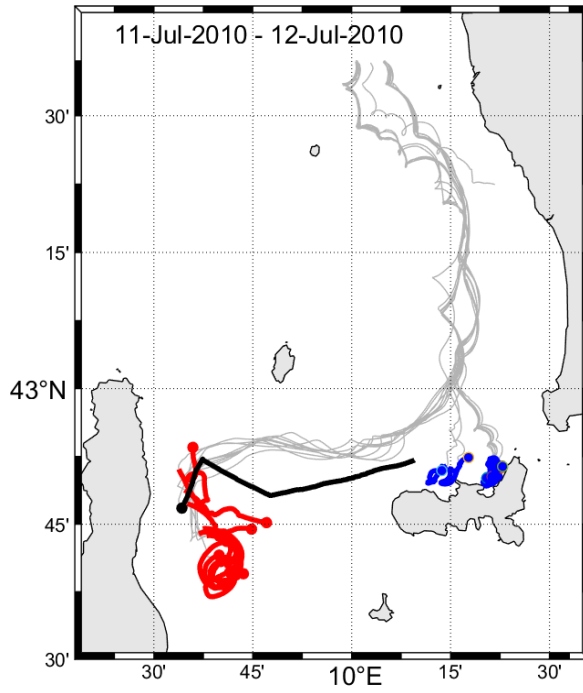
596

597

598

599

Figure 2. Two-day long drifter (red: coastal group; blue: outer group; green: intermediate drifter) and glider (black) track segments, with dot corresponding to the end of the second day, between 3 and 20 July. Cumulative tracks are shown in light grey shade.



600

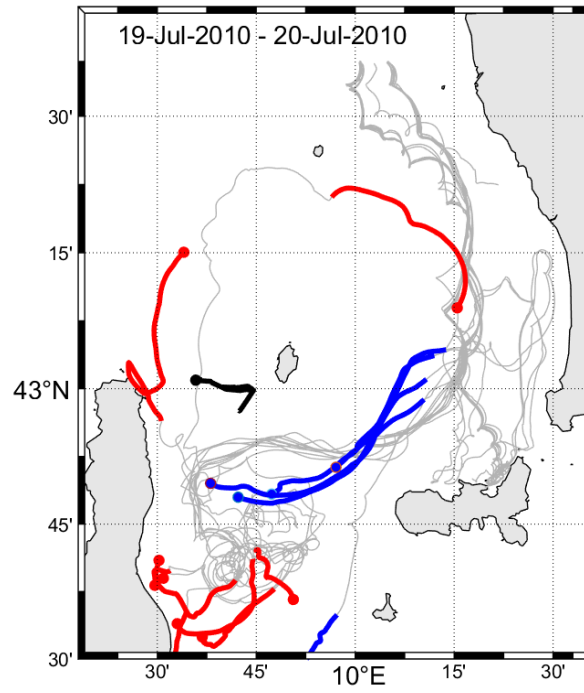
601

602

603

604

Figure 2. Continued.



605  
606

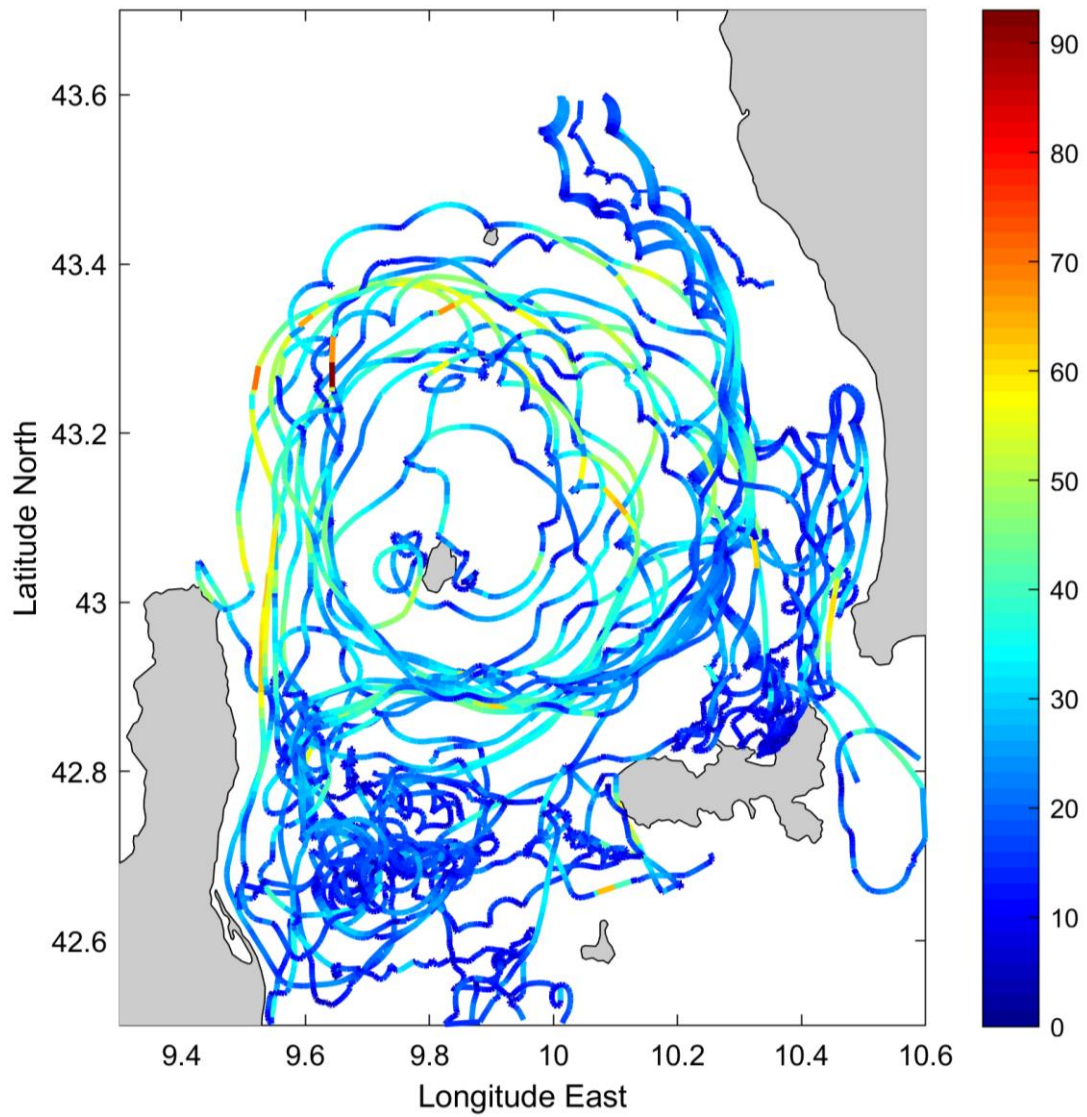
607

608

609

Figure 2. Continued.

610



611

612 Figure 3. Drifter trajectories for the period 3 July – 27 August 2010 color-coded as a function

613 of drifter speed (cm/s).

614

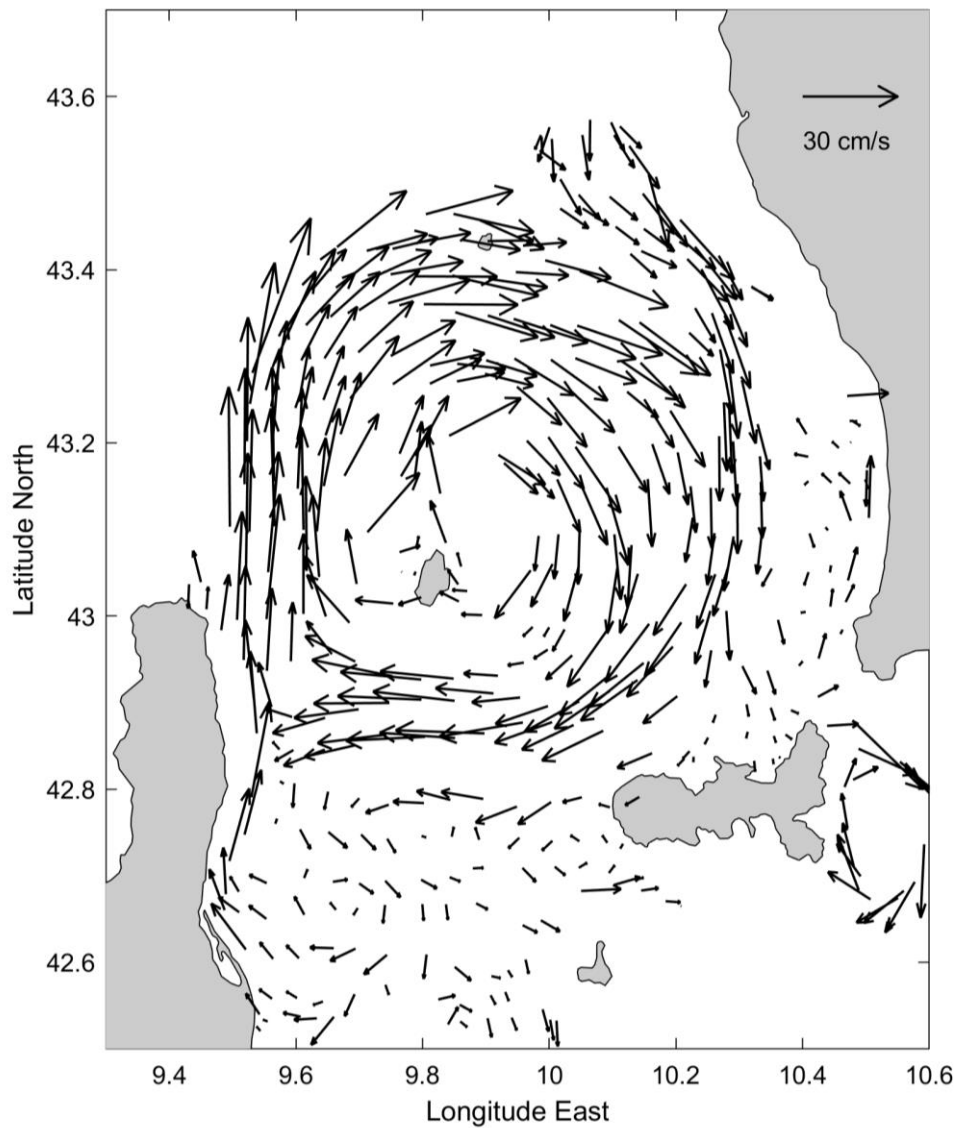
615

616

617

618

619



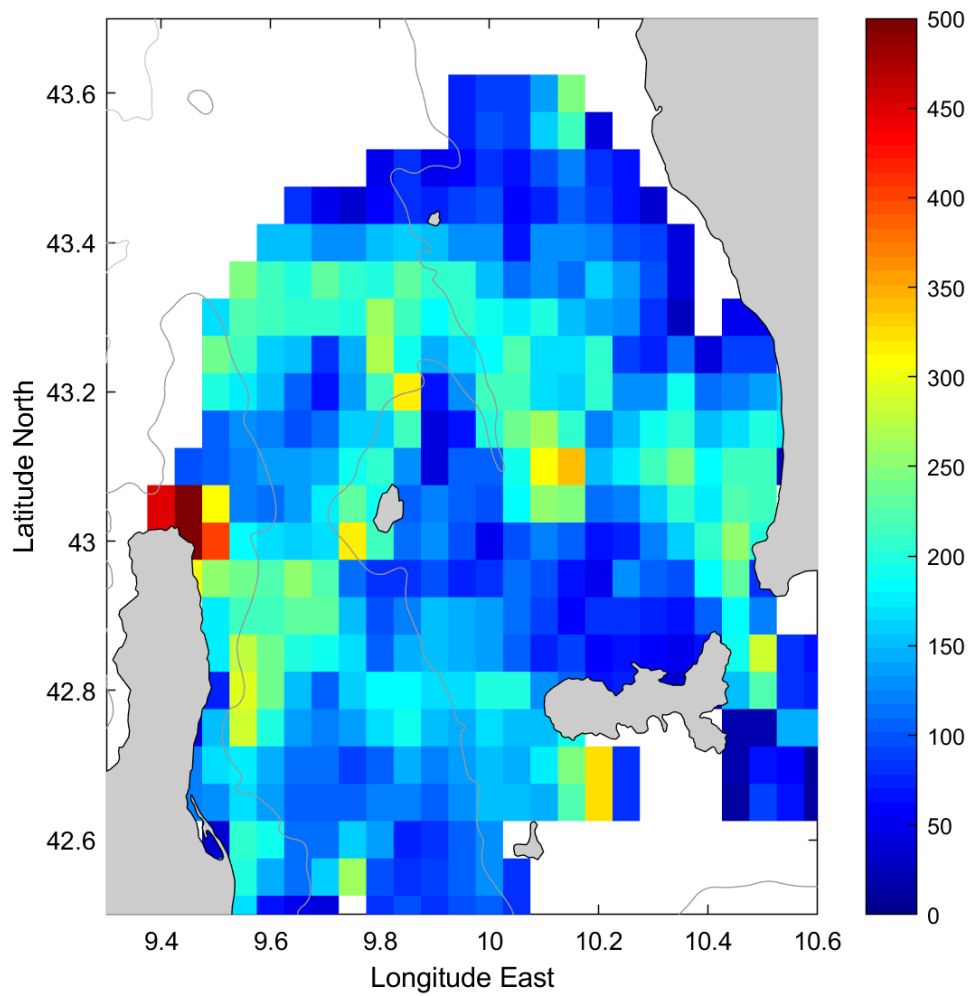
621

622

623 Figure 4. Mean surface circulation (arrows) and mean kinetic energy (colors,  $\text{cm}^2/\text{s}^2$ ) in study  
624 area for the period 3 July – 27 August 2010 using bins of  $0.05^\circ \times 0.05^\circ$ . Bins with less than 5  
625 hourly observations were omitted.

626

627



629

630 Figure 5. Kinetic energy per unit mass of the velocity residuals or eddy kinetic energy (EKE,  
 631  $\text{cm}^2 \text{s}^{-2}$ ) in study area for the period 3 July – 27 August 2010 using bins of  $0.05^\circ \times 0.05^\circ$ . Bins

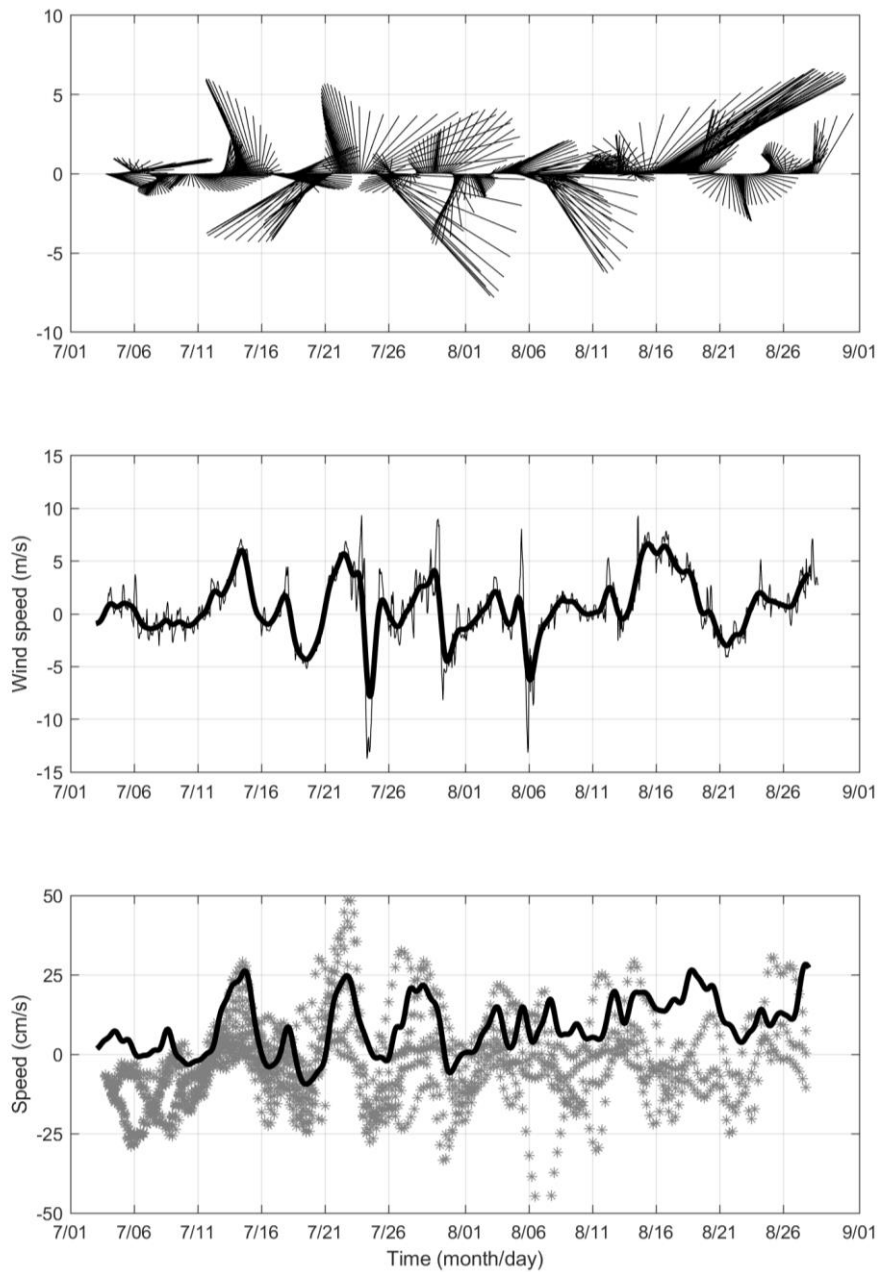
632

with less than 5 hourly observations were omitted.

633

634

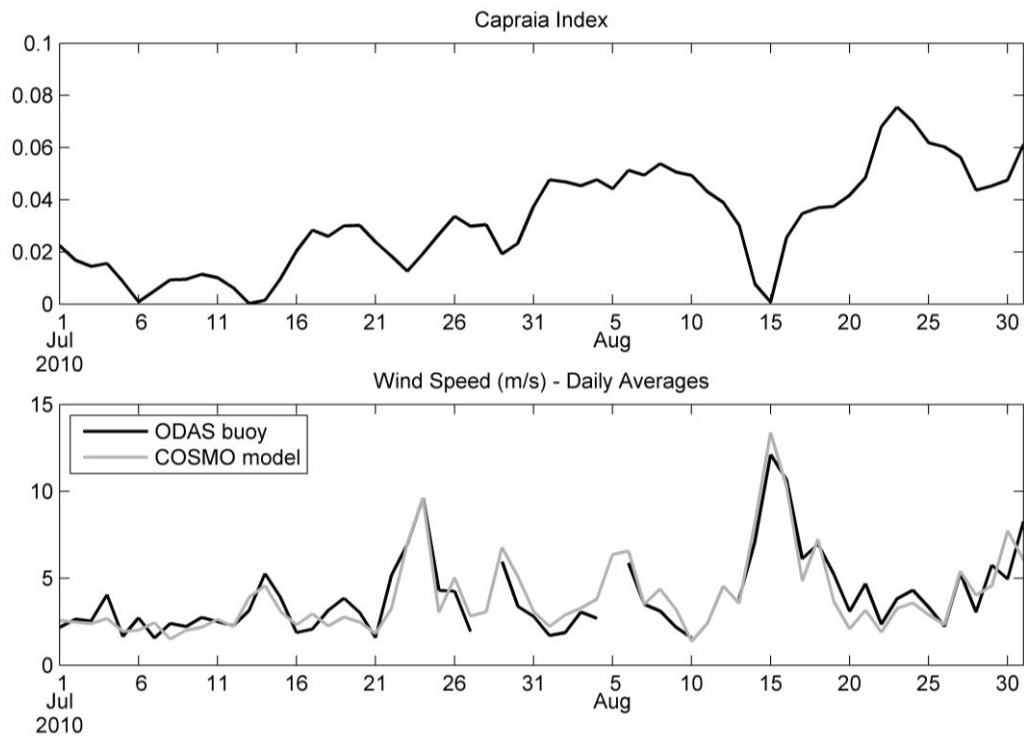
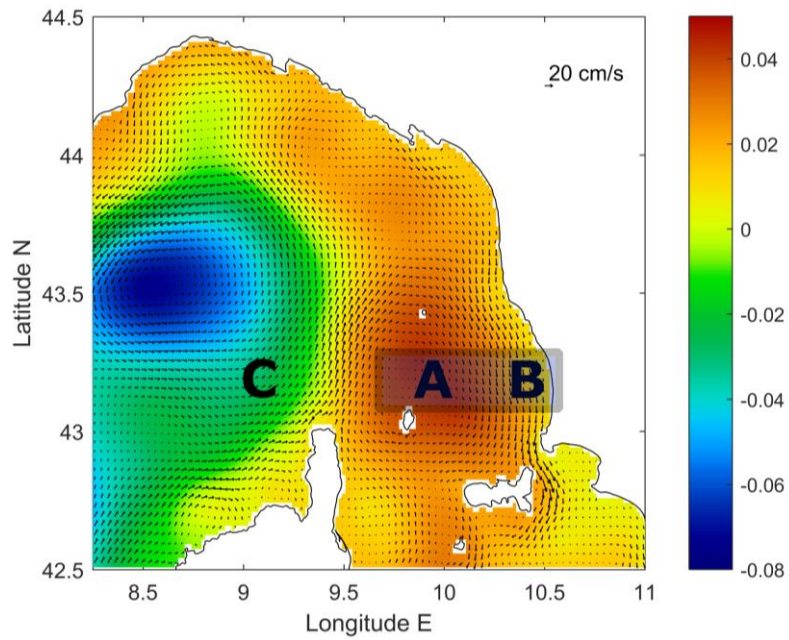
635



636

637 Figure 6. Stick diagram of the low-pass filtered COSMO-ME 10-m winds at grid point  $43^{\circ}$   
 638  $7.5^{\circ}$  N,  $9^{\circ} 37.5^{\circ}$  E in the CC between 3 July and 27 August 2010 (top panel). Full (thin curve)  
 639 and low-pass filtered (tick curve) COSMO-ME 10-m wind meridional component at the same  
 640 location (middle panel). Low-pass filtered near-surface velocities at 32 m in the CC from  
 641 mooring data (thick curve) and low-pass filtered velocities (light grey stars) of all the drifters  
 642 in the study area (bottom panel).

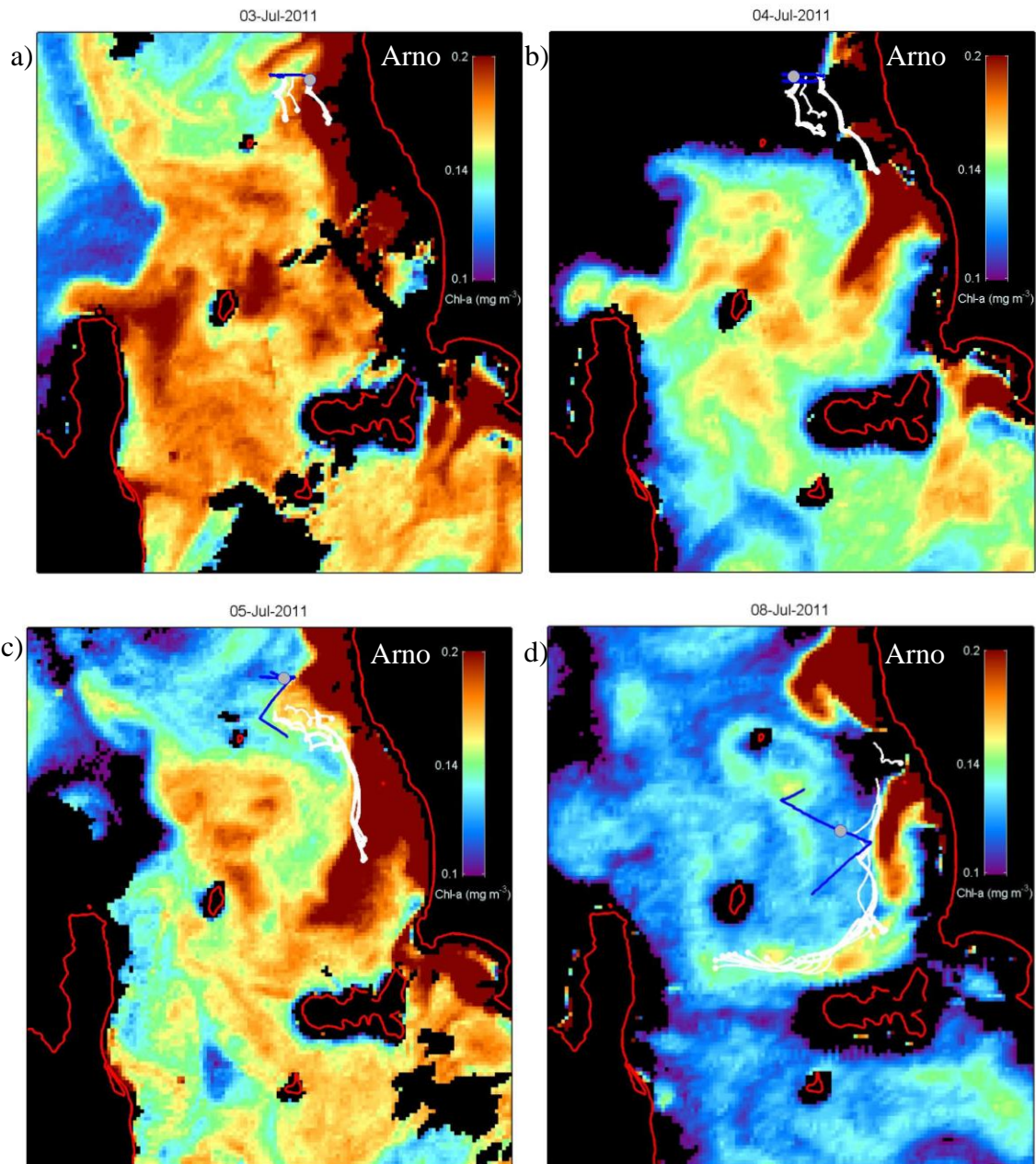
643



644

645 Figure 7. Ligurian Sea average circulation in July-August 2010 as simulated by ROMS (top  
 646 panel). Colour is sea surface height (m) and arrows surface currents. Evolution of the daily  
 647 average of the Capraia Index (m; middle panel) confronted to the daily average of COSMO-  
 648 ME 10-m wind speed (m/s) at the ODAS buoy location and the measured ODAS 10-m wind  
 649 speed (bottom panel).

650



651

652

653

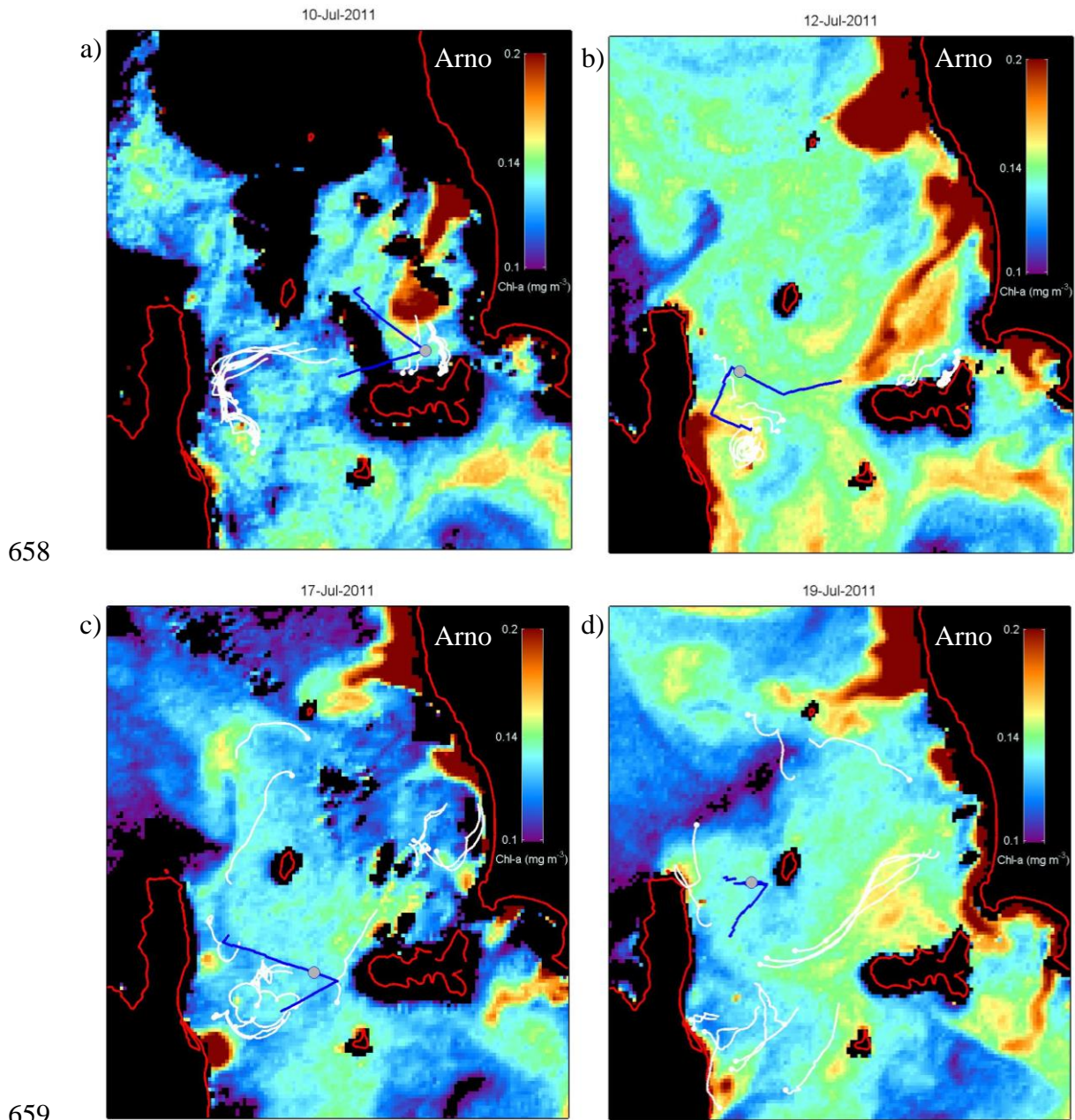
654

655

656

657

Figure 8. MODIS images of chlorophyll concentration on 3, 4, 5 and 8 July 2010, superimposed with centered 2-day long trajectories of drifters (white) and glider (blue). The gray dot represents the location of the glider at 12 GMT, contemporaneous with the satellite images.



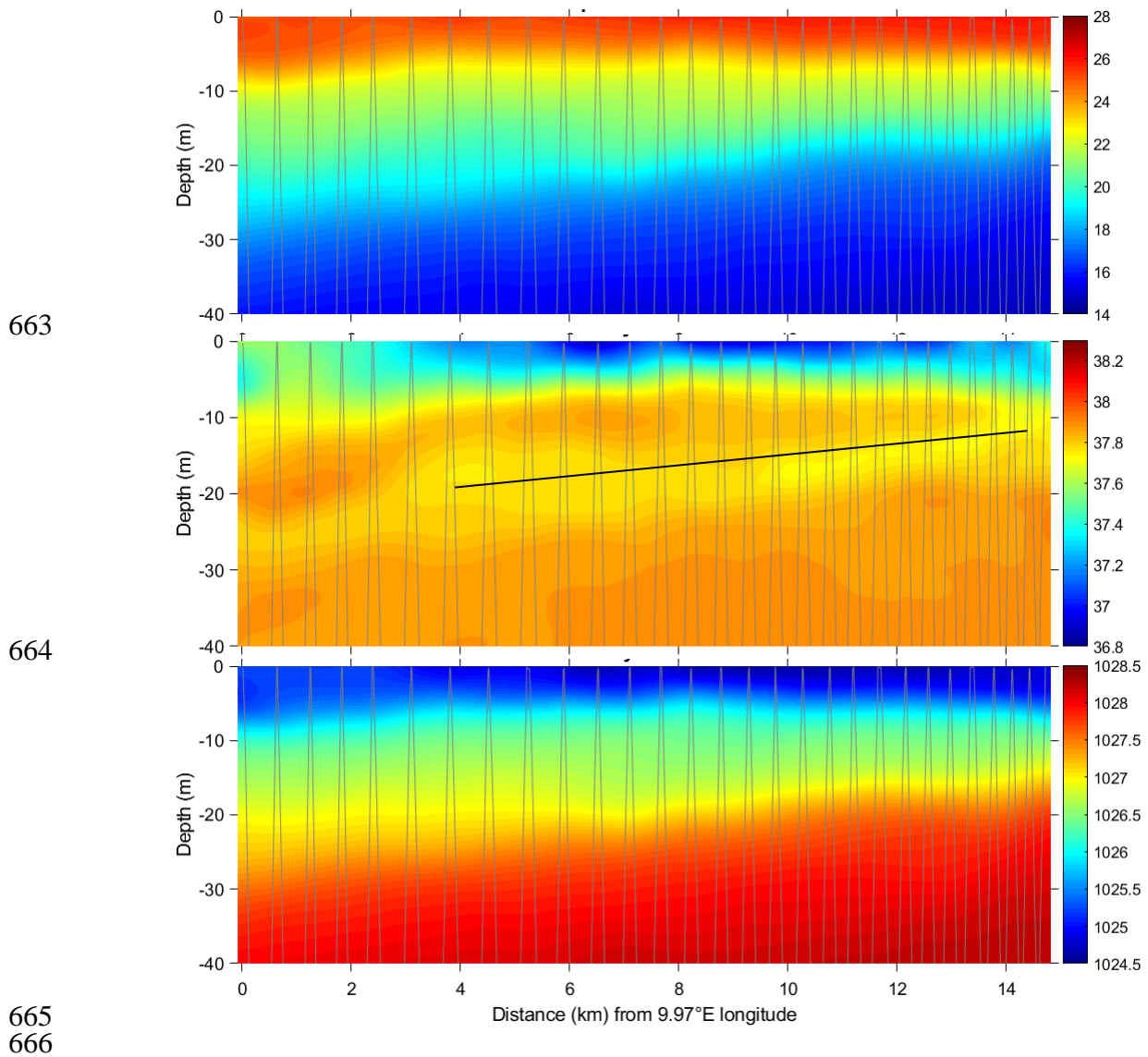
659

660

661

662

Figure 9. Same as Figure 8 but for 10, 12, 17 and 19 July 2010.



667 Figure 10. Contour plots of temperature ( $^{\circ}\text{C}$ , top), salinity (middle) and density ( $\text{kg}/\text{m}^3$ ,  
 668 bottom) versus depth and horizontal distance along glider transect 1. The origin is the  
 669 westernmost location and the glider yo-yo track is shown with light grey lines. In the middle  
 670 panel, a black line indicate subduction of less saline water along the isopycnals.

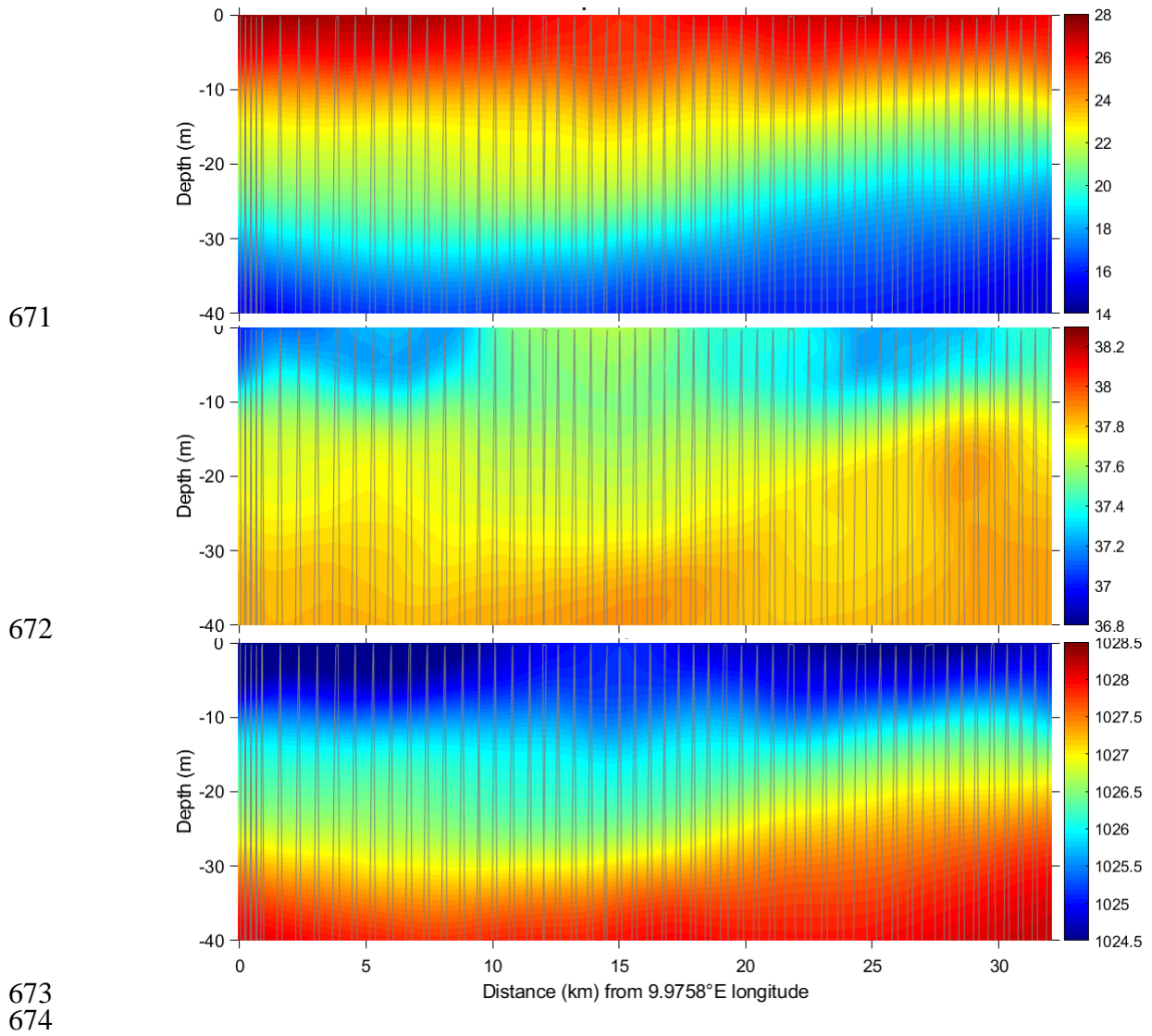


Figure 11. Same as in Figure 10 but for glider transect 8.

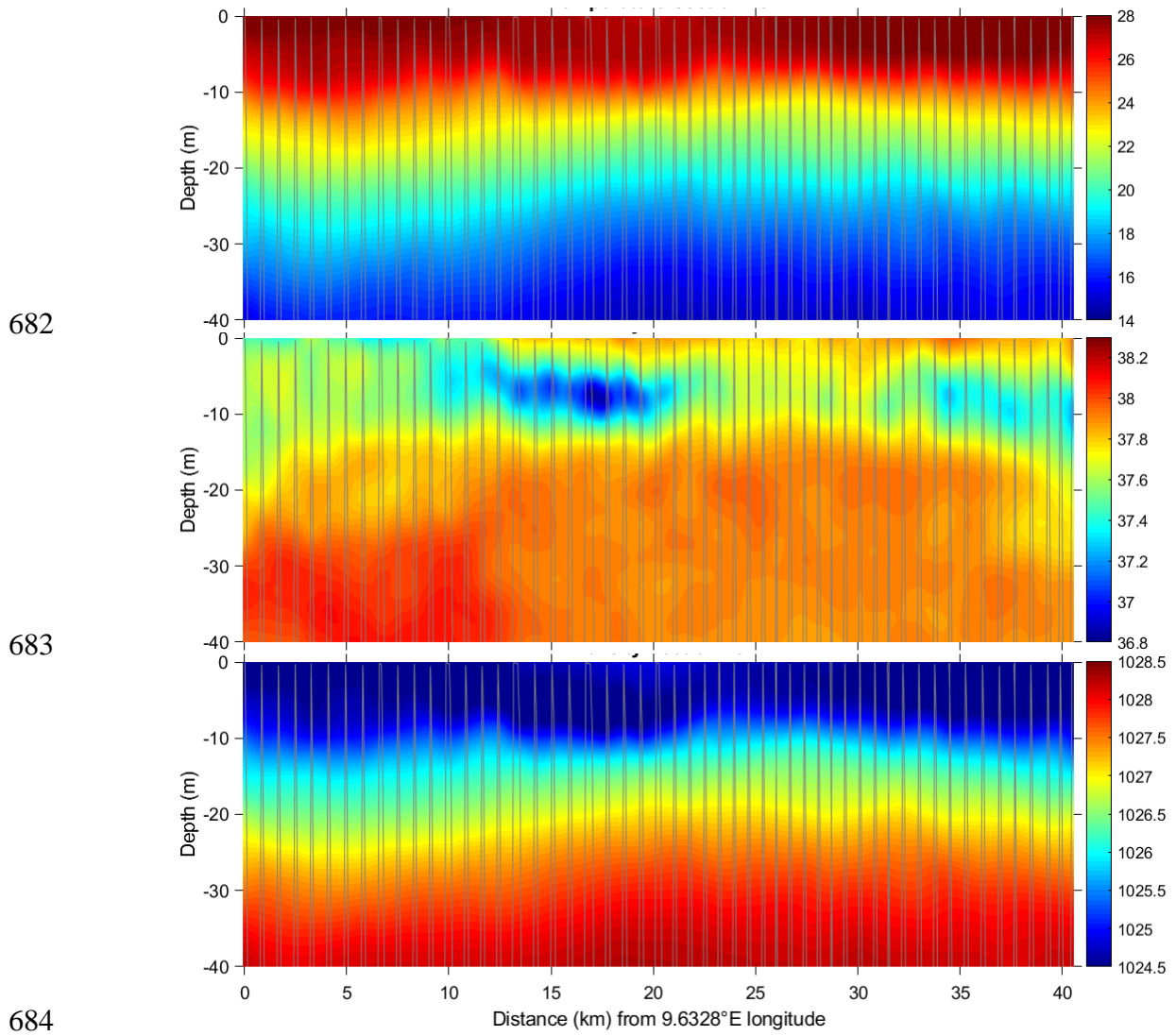
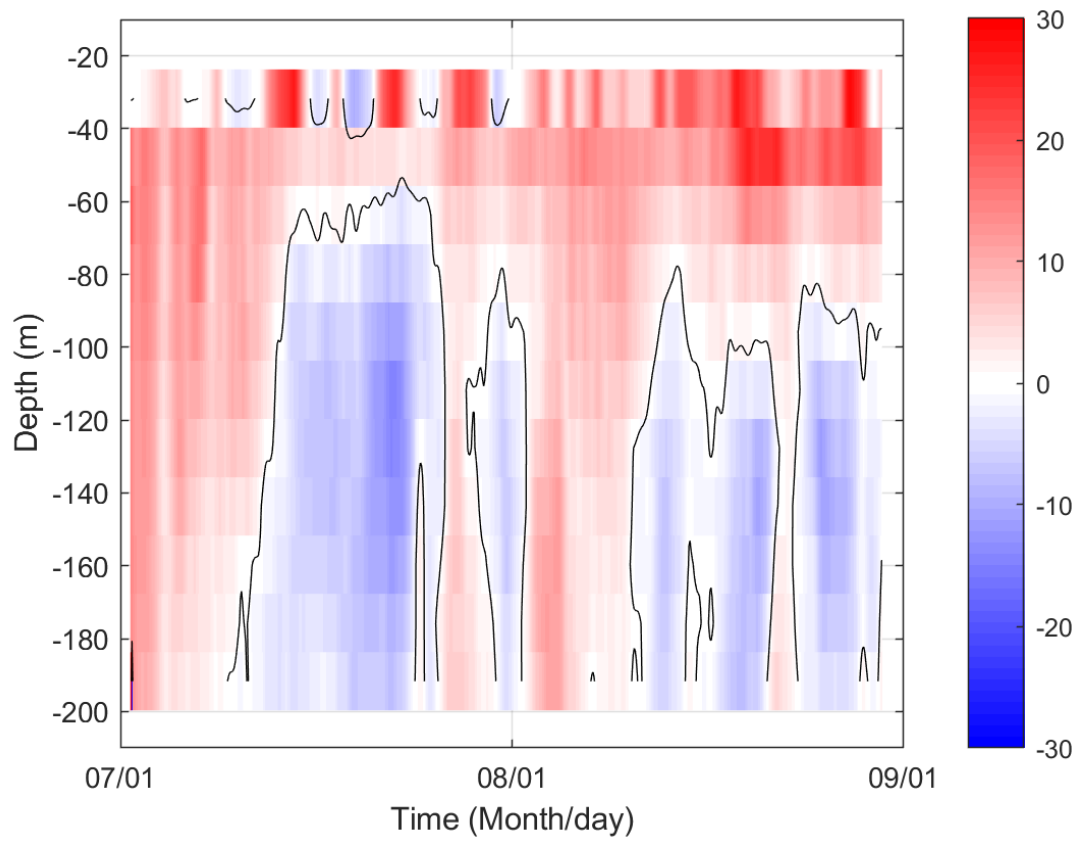


Figure 12. Same as in Figure 10 but for glider transect 15.



687

688

689 Figure 13. Meridional velocity (cm/s) measured by the moored ADCP in the CC (positive  
 690 northward) as a function of time and depth above 200 m depth. The uppermost ADCP cell  
 691 was excluded. The null value is contoured with black curves.

692

693

694